

Modeling of crystal dissolution of poly(vinyl alcohol) gels produced by freezing/thawing processes

C.M. Hassan¹, J.H. Ward, N.A. Peppas*

Polymer Science and Engineering Laboratories, School of Chemical Engineering, Purdue University, West Lafayette, IN 47907-1283, USA

Received 21 May 1999; received in revised form 16 December 1999; accepted 22 December 1999

Abstract

A model was developed to describe the overall dissolution kinetics of semicrystalline PVA gels prepared by freezing and thawing techniques. The dissolution process was described as a three-step mechanism: detachment-, diffusion-, and disentanglement-controlled dissolution. The unfolding of crystalline regions due to detachment and diffusion was calculated. The lamellar thickness of a PVA crystal was found to significantly change the rate of unfolding and thus, the overall dissolution kinetics. The model predicted the effect of the lamellar thickness, time of swelling, and sample thickness on the crystal chain unfolding and potential dissolution of freeze/thawed PVA hydrogels. © 2000 Elsevier Science Ltd. All rights reserved.

Keywords: Polymer dissolution; Poly(vinyl alcohol); Disentanglement

1. Introduction

Poly (vinyl alcohol) (PVA) hydrogels prepared by freezing and thawing techniques have demonstrated a great potential for various applications due to certain properties that are preferable to those of gels prepared by traditional crosslinking techniques [1]. The most notable properties include their lack of toxicity and increased mechanical strength. Freeze/thawed PVA gels are prepared by exposing aqueous PVA solutions to repeated cycles of freezing at -20°C and thawing at room temperature. This procedure results in the formation of crystallites that serve as physical crosslinks to render the material insoluble in water. However, with such semicrystalline materials, there is still significant change in the overall crystalline structure during the initial swelling process. Of particular interest is the melting out of smaller crystalline regions and the subsequent dissolution of PVA.

The appropriateness of PVA hydrogels for various biomedical applications has been recognized because of their high water content and rubbery nature [2]. In particular, PVA hydrogels prepared by freezing and thawing techniques show enhanced mechanical strength and have been

examined for use as intervertebrate disc nuclei [3], artificial articular cartilage [4], and as a contact lens material [5–7]. When considering such applications, specifically over extended periods of time, changes in the crystalline structure must be accurately predicted.

The dissolution of semicrystalline polymers has been described previously by Mallapragada and Peppas [8]. A mathematical model based on free energy changes during the crystal unfolding and disentanglement process was proposed to predict the overall dissolution kinetics. The model was based on a uniform crystal size and provided reasonable predications for the dissolution of semicrystalline PVA (prepared by annealing at high temperatures) in water.

However, when considering PVA gels prepared by freezing and thawing techniques, a better understanding of the dissolution process must be obtained to predict the overall dissolution kinetics. In particular, the crystalline nature of PVA, the potential of PVA dissolution, and the overall long-term stability of the system are key issues. Therefore, in the present work, the distribution of crystal size was a critical issue in accurately modeling the overall crystal chain unfolding and potential dissolution of freeze/thawed PVA hydrogels.

2. Experimental

2.1. PVA gel preparation

Various experimental techniques were implemented in

* Corresponding author. Tel.: +1-765-494-7944; fax: +1-765-494-4080.

E-mail address: peppas@ecn.purdue.edu (N.A. Peppas).

¹ Present address: Westvaco, Inc., Laurel Technical Center, 11101 Johns Hopkins Road, Laurel, MD 20723-6006, USA.

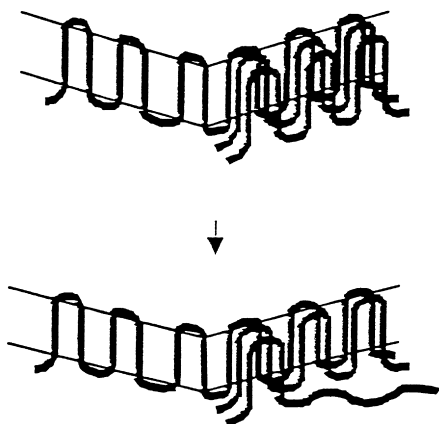


Fig. 1. Detachment-controlled dissolution.

order to examine the dissolution of semicrystalline PVA gels prepared by freezing and thawing techniques. Aqueous solutions of PVA were first prepared by dissolving PVA (Elvanol[®] HV, E.I. DuPont de Nemours, Wilmington, DE, $\bar{M}_n = 64\,000$, polydispersity index = 2.02, degree of hydrolysis = 99.0%) in deionized water for 6 h at 90°C. The solutions were cast between glass microscope slides with 0.7 mm thick spacers. PVA gels were then produced by exposing the solutions to three cycles of freezing for 8 h at -20°C and thawing for 4 h at 25°C.

2.2. Dissolution studies

The dissolution of PVA gel samples prepared as indicated above was conducted at 37°C in jars containing 50 ml of distilled/deionized water. Dissolved PVA was determined by complexing a 5 ml sample of aqueous PVA with 2.5 ml of a 0.65 M boric acid solution and 0.3 ml of a 0.05 M I₂/0.15 M KI solution and then diluting to 10 ml with

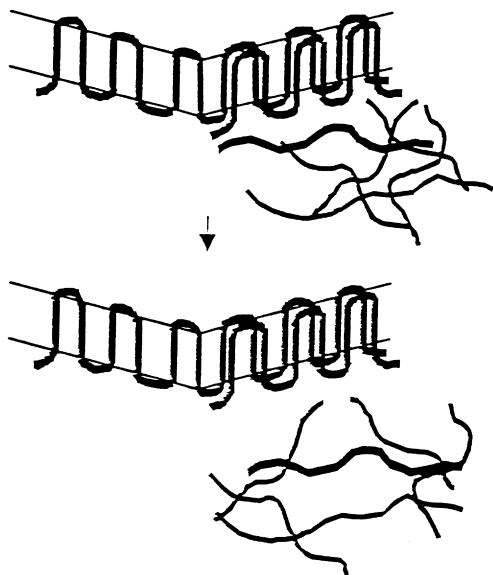


Fig. 2. Diffusion-controlled dissolution.

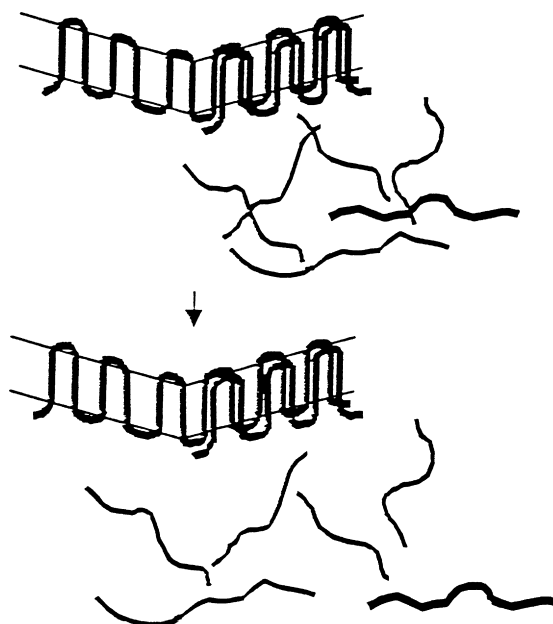


Fig. 3. Disentanglement-controlled dissolution.

deionized water at 25°C. The absorbance of visible light at 671 nm was then measured to determine the concentration of complexed PVA in solution.

2.3. Characterization of PVA hydrogels

Differential scanning calorimetry (DSC, model 2910, TA Instruments, New Castle, DE) was used to determine the degrees of crystallinity and crystal size distributions of samples in the initial state (before swelling) and at various times during swelling in deionized water at 37°C. In a typical experiment, 5–10 mg of a dried sample was placed in an aluminum pan and heated at a scanning rate of 5°C/min from 30 to 250°C. A nitrogen purge through the sample chamber was implemented to obtain a more uniform, stable thermal environment.

3. Theoretical model of polymer dissolution

Semicrystalline PVA samples produced by freezing/thawing techniques dissolve by unfolding of the crystal chains to join the amorphous portion, followed by subsequent disentanglement.

The process of crystal dissolution may be expressed in terms of a series of steps/mechanisms. First, a chain belonging to a crystal is detached from the crystal in the presence of water (detachment-controlled dissolution; Fig. 1). Then, in a second step, the chain diffuses through the amorphous PVA samples, while the water concentration, v_1 , increases progressively (diffusion-controlled dissolution; Fig. 2). Finally, the chain passes through a disentanglement process and dissolves (disentanglement-controlled dissolution; Fig. 3).

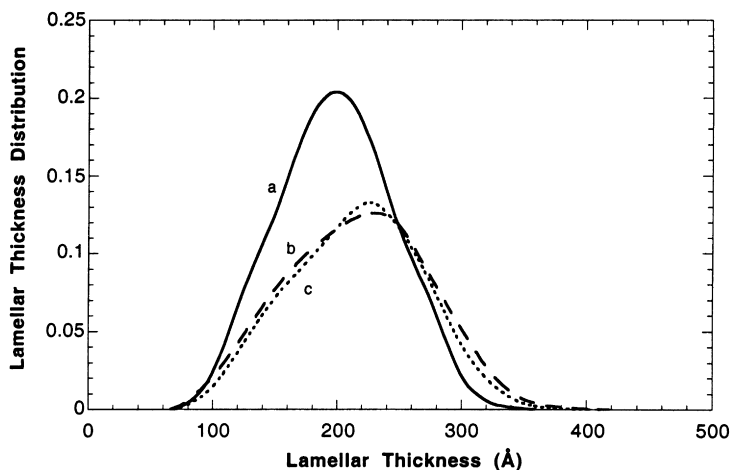


Fig. 4. Crystal size distributions in the initial state (a); after 1 day of swelling (b); and after 15 days of swelling (c); for PVA samples prepared with $\bar{M}_n = 64\,000$ and three cycles of 8 h freezing and 4 h thawing and concentration of 15 wt%.

Both the crystal unfolding (detachment-controlled or diffusion-controlled) as well as the disentanglement process can be modeled in order to predict the kinetics of the process. Here, we are developing first a model to determine the unfolding rate (or kinetic constant) during crystallite PVA dissolution. Then, this unfolding parameter is used to model the overall dissolution kinetics using a diffusion-based model.

3.1. Unfolding (detachment/diffusion) of crystal chains for semicrystalline, freeze/thawed PVA gels

In freeze/thawed gels, crystallite formation occurs due to the folding of PVA chains. It is then evident that the free energy change during chain unfolding will depend on the dimensions of the crystals and on the surface energies along different planes in the crystal. Semicrystalline freeze/thawed PVA gels were found to contain a distribution of crystallites ranging from 50 to 400 Å, which changes during the dissolution process. A typical crystal size distribution obtained from a PVA sample prior to swelling and after 1 and 15 days of swelling is shown in Fig. 4. As the PVA chains of the crystals unfold by detachment and diffusion to join the amorphous PVA structure, they interact with water. The Gibbs free energy change during this dissolution process can be attributed to the thermodynamic mixing of PVA and water and is given by the Flory–Huggins equation.

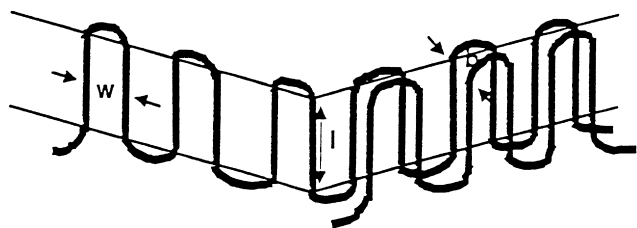


Fig. 5. Representation of a typical crystallite of lamellar thickness, l , width, w , and distance, b , between rows of chains.

Obviously, in the relevant equations, the tie-points of the classical theory are replaced by the crystallites, while hydrogen bonding forces are ignored.

We consider a thin slab of semicrystalline PVA gels containing a range of crystallites. A typical crystallite is described as consisting of folded polymer chains (see Fig. 5) of lamellar thickness l , width w , and distance b between the rows of chains, and having a cross-sectional area a . As we have shown in our experimental studies, the lamellar thickness, l , varies with preparation techniques (i.e. with the freezing/thawing conditions). Thus, the initial crystalline phase has a wide crystal size distribution. We can now express the Gibbs free energy change ΔG_1 of unfolding a segment of chain of length l , thickness b and width w from a single crystal

$$\Delta G_1 = bwl\Delta f - 2bw\sigma_e - 2bl\sigma_s \quad (1)$$

Here, Δf indicates the Gibbs free energy difference per unit volume of PVA chains between the crystalline and amorphous phases of PVA and σ_e and σ_s are the free energies expressed per end and side surfaces, respectively. Thus, Eq. (1) can be used to calculate the change of Gibbs free energy of simply unfolding a chain segment from ν successive chains in a crystal. The parameter ν is the number of successive chains that form a crystal.

If the crystalline chain detachment is done in a way such that $(\nu + 1)$ rows of chains are transformed into ν rows, then Eq. (1) can be rewritten with $\sigma_e = \sigma_s$ as follows:

$$\Delta G_{\nu+1} - \Delta G_\nu = bw(l\Delta f - 2\sigma_e) \quad (2)$$

The additional contribution to the dissolution process is from the Gibbs free energy of mixing once the unfolded PVA chains available in the amorphous phase mix with water. This free energy, ΔG_{mix} , can be expressed according to the Flory–Huggins theory as

$$\Delta G_{\text{mix}} = kT(n_1 \ln v_1 + n_{2a} \ln v_{2a} + \chi n_1 v_{2a}) \quad (3)$$

where v_1 is the water volume fraction, v_{2a} is the amorphous PVA volume fraction, n_1 and n_2 are the moles of water and PVA, respectively, and χ is the Flory PVA–water interaction parameter that has been reported in the literature by Peppas and Merrill [9] as 0.494.

Then, clearly the overall crystal chain dissolution process can be associated to the change of the Gibbs free energy

$$\Delta G_{\text{tot}} = \Delta G_{\nu+1} - \Delta G_{\nu} + \Delta G_{\text{mix}} \quad (4)$$

Crystal dissolution is a rate process and as such it is governed by the classic Eyring theory of rate processes [10]. According to it, the rate process is proportionally related to the exponential forces of enthalpic and entropic changes as dictated by the Gibbs free energy. For a PVA crystal dissolution process, the overall rate of the crystal dissolution process, i.e. the overall rate of the crystal dissolution from initial crystals of ν successive chains per crystal is

$$R(\nu, l) = N(\nu + 1, l) \frac{kT}{h} \exp\left(-\frac{\Delta G_{\text{tot}}}{kT}\right) \quad (5)$$

Here, $N(\nu + 1, l)$ indicates the number of crystals containing $\nu + 1$ successive chains and having lamellar size l , and dissolving to $N(\nu, l)$ crystals containing ν chains of size l , at a net “loss” of one crystalline chain. Also, k is the Boltzmann constant, and h is the Planck constant. From this expression, the final form of the rate expression is:

$$R(\nu, l) = N(\nu + 1, l) \frac{kT}{h} \exp\left[-\frac{bw(l\Delta f - 2\sigma_e)}{kT}\right] \times \exp[-(n_1 \ln v_1 + n_{2a} \ln v_{2a} + \chi n_1 v_{2a})] \quad (6)$$

From this expression, the rate constant of PVA chain unfolding can be written as:

$$k_1 = \frac{kT}{h} \exp\left[-\frac{bw(l\Delta f - 2\sigma_e)}{kT}\right] \exp[-(n_1 \ln v_1 + n_{2a} \ln v_{2a} + \chi n_1 v_{2a})] \quad (7)$$

Typical values of the parameters in the above equation have been tabulated [11] as σ_e of 100 erg/cm² and σ_s of 10 erg/cm². The term Δf may also be calculated [5] by using the following equation:

$$\Delta f = \frac{\Delta h_f(T_m^0 - T)}{T_m^0} \quad (8)$$

where Δh_f is the heat of fusion per unit volume of PVA, T_m^0 is the melting point of an infinitely thick PVA crystal, and T is the dissolution temperature. The value of Δh_f has been reported [12] as 303 J/cm³. The value of T_m^0 depends on the molecular weight of PVA and its calculation followed the analysis of Peppas and Hansen [13]. The value of T_m^0 was 516.5 K for PVA with $\bar{M}_n = 64\,000$.

Eq. (6) shows that the rate constant of chain unfolding is a function of:

1. the chain dissolution temperature, T ;
2. the number, N , and initial size, l , of crystals;
3. the energetic characteristics, σ_e , of the PVA crystal;
4. the compatibility of PVA with water as judged by the value of χ ; and
5. the water volume fraction, v_1 .

Some interesting qualitative conclusions can be drawn from the form of Eq. (6). Clearly, small crystals lead to high dissolution rates. This is observed in our own dissolution analysis (see Fig. 4) where the small crystals dissolve early in the dissolution process.

The effect of the lamellar thickness of crystals in freeze/thawed PVA gels on the unfolding rate was examined in more detail. A specific sample, with its corresponding range of crystal lamellar thickness, was used for such an analysis. The values used were representative of PVA gels that were prepared from an initial solution of 15 wt%, contained a PVA molecular weight of $\bar{M}_n = 64\,000$, and were exposed to three cycles of freezing and thawing. Such gels were previously shown in Fig. 4 to have crystals ranging from 50 to 400 Å. However, the origin of Eq. (6) was based on a very narrow distribution of crystals [11]. Therefore, the range of crystals examined in the present analysis (185–215 Å) included the peak lamellar thickness $\pm 7.5\%$ of the peak value. Such a range was in agreement with the original derivation of this analysis of the rate of unfolding.

The rate of unfolding as a function of the lamellar thickness is shown in Fig. 6. It is apparent that the rate of unfolding of PVA chains is significantly impacted by the lamellar thickness of the crystal. Essentially, the crystals of lower lamellar thickness of 185 Å unfold faster than crystals with a lamellar thickness of 215 Å by nearly three orders of magnitude. These results indicate that when examining the overall dissolution kinetics of PVA gels prepared by freezing and thawing techniques, it is crucial to consider the distribution of the crystals present in the initial gel structure.

The effect of both the water volume fraction and the degree of crystallinity on the rate of unfolding were also examined. However, very little variation was observed in the unfolding rate over the range of interest for these parameters. Therefore, only the effect of the lamellar thickness on the unfolding rate was considered further in modeling the overall dissolution kinetics of freeze/thawed PVA gels.

3.2. Model of overall dissolution kinetics of semicrystalline polymers

Now, the overall dissolution kinetics can be modeled by incorporating the rate of PVA chain unfolding, $R(\nu + 1, l)$, into a continuum framework based on a semicrystalline polymer slab of half thickness L_0 .

The PVA film is assumed to consist of crystalline PVA, v_{2c} , amorphous PVA, v_{2a} , and water v_1 . The amorphous

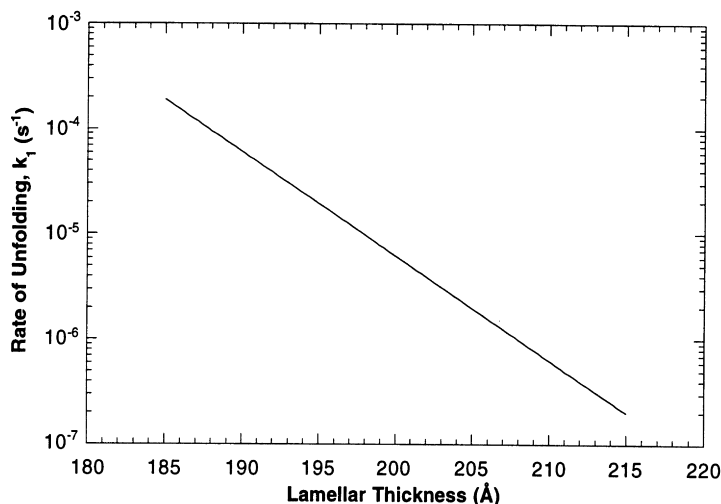


Fig. 6. Rate of unfolding as a function of lamellar thickness.

PVA portion is in the glassy state but the glassy/rubbery transition kinetics is assumed to be very fast in comparison to the dissolution kinetics. This is a reasonable assumption for the dissolution of very thin PVA films. Water transport is assumed to be one-dimensional. Water penetrates the film, causing unfolding of the crystalline chains (by detachment and diffusion) and increases the amorphous portion of PVA. The three diffusants in the system are water, amorphous PVA, and crystalline PVA; their properties are indicated by the suffixes 1, 2a and 2c, respectively.

Expressions were written for the rates of change of volume fractions, v , of the various components where the sum of the three volume fractions was always equal to unity. The change of crystalline PVA, v_{2c} , is written as being proportional to the unfolding rate, k_1 , and the water concentration:

$$\frac{\partial v_{2c}}{\partial t} = -k_1 v_1 \quad (9)$$

The change of amorphous PVA may be expressed by a classical diffusion equation with an additional term because of the transformation of the crystalline PVA into amorphous PVA during the unfolding process.

$$\frac{\partial v_{2a}}{\partial t} = \frac{\partial}{\partial x} \left(D \frac{\partial v_{2a}}{\partial x} \right) + k_1 v_1 \quad (10)$$

The amorphous PVA diffusion coefficient, D , was assumed to be dependent on the water volume fraction according to the equation proposed by Fujita [14]:

$$D = D_0 \exp(a_D v_1) \quad (11)$$

Here, D_0 is the self diffusion coefficient of PVA and a_D is a constant that represents the abrupt diffusional change of the glassy–rubbery transition. The values of D_0 and a_D have been reported by Fujita [14] as $10^{-5} \text{ cm}^2/\text{s}$ and 7, respectively.

The initial and boundary conditions of this system are

shown as follows. Initially, the gel contains specific amorphous and crystalline volume fractions, v_{2a0} and v_{2c0} , respectively.

$$t = 0 \quad -L_0 \leq x \leq L_0 \quad v_{2a} = v_{2a0} \quad (12a)$$

$$t = 0 \quad -L_0 \leq x \leq L_0 \quad v_{2c} = v_{2c0} \quad (12b)$$

A symmetry condition at the center of the slab was represented as

$$t > 0 \quad x = 0 \quad \frac{\partial v_{2a}}{\partial x} = 0 \quad (13)$$

To complete the system, a value for the volume fraction of water at the polymer–solvent interface was chosen which was representative of the volume fraction of water at dissolution, v_{diss} . This parameter was specified so as not to violate the mass balance of the system.

$$t > 0 \quad x = \pm L \quad v_1 = v_{\text{diss}} \quad (14)$$

The problem was solved with these initial and boundary conditions to describe the chain unfolding and dissolution of freeze/thawed PVA hydrogels. From this model, profiles for the crystalline and amorphous volume fractions as a function of time were obtained. In particular, the effect of varying the lamellar thickness was examined to gain insight as to the overall dissolution kinetics of a PVA sample with a broad distribution of crystals. The model predictions were compared with the experimental results for swelling PVA gels prepared by freezing/thawing techniques.

3.3. Solution technique

The system of partial differential equations was solved numerically using explicit and implicit finite difference techniques. The x coordinate is represented by the subscript i and time is represented by the superscript n . The spatial step is Δx and the time step is Δt . The transformed equations

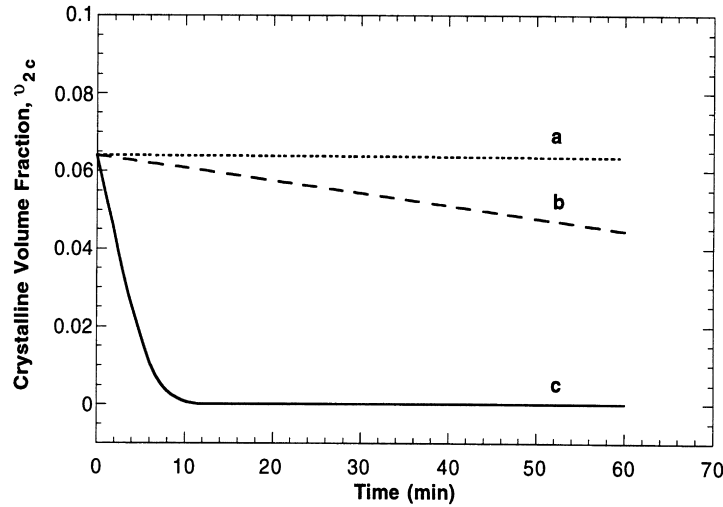


Fig. 7. Crystalline volume fraction as a function of time for samples containing crystals of lamellar thickness of (a) 215 Å; (b) 200 Å; and (c) 185 Å.

in finite difference form are shown.

$$\frac{v_{2c,i}^{n+1} - v_{2c,i}^n}{\Delta t} = -k_1(1 - v_{2c,i}^n - v_{2a,i}^n) \quad (15)$$

$$\begin{aligned} \frac{v_{2a,i}^{n+1} - v_{2a,i}^n}{\Delta t} = & k_1(1 - v_{2a,i}^n - v_{2c,i}^n) \\ & + p_i^n \left(\frac{v_{2a,i+1}^{n+1} - 2v_{2a,i}^{n+1} + v_{2a,i-1}^{n+1}}{\Delta x^2} \right) \\ & - a_D p_i^n \left(\frac{v_{2a,i+1}^n - v_{2a,i-1}^n}{2\Delta x} + \frac{v_{2c,i+1}^n - v_{2c,i-1}^n}{2\Delta x} \right) \\ & \times \left(\frac{v_{2a,i+1}^n - v_{2a,i-1}^n}{2\Delta x} \right) \end{aligned} \quad (16)$$

where

$$p_i^n = D_0 \exp(a_D(1 - v_{2a,i}^n - v_{2c,i}^n)) \quad (17)$$

Eq. (16) was then recast into a tridiagonal form as shown

$$\begin{aligned} v_{2a,i-1}^{n+1} \left(-\frac{p_i^n}{\Delta x^2} \right) + v_{2a,i}^{n+1} \left(\frac{1}{\Delta t} + \frac{2p_i^n}{\Delta x^2} \right) + v_{2a,i+1}^{n+1} \left(-\frac{p_i^n}{\Delta x^2} \right) \\ = \frac{v_{2a,i}^n}{\Delta t} - a_D \left(\frac{v_{2a,i+1}^n - v_{2a,i-1}^n}{2\Delta x} + \frac{v_{2c,i+1}^n - v_{2c,i-1}^n}{2\Delta x} \right) \\ \times \left(\frac{v_{2a,i+1}^n - v_{2a,i-1}^n}{2\Delta x} \right) + k_1(1 - v_{2a,i}^n - v_{2c,i}^n). \end{aligned} \quad (18)$$

4. Results and discussion

Values representative of a typical PVA gel prepared by freezing and thawing techniques were used in simulations to predict the overall dissolution kinetics of the system. A PVA sample prepared from an initial aqueous concentration of 15 wt%, a molecular weight of $M_n = 64\,000$, and three

cycles of freezing and thawing, as indicated in the experimental section, was used as the model system. It was determined that this system initially contained a volume swelling ratio of approximately 8, a degree of crystallinity of 52%, and crystals ranging from 50 to 400 Å with a peak lamellar thickness at 200 Å.

As described previously, the range of crystals examined in modeling the dissolution kinetics was narrowed to the peak lamellar thickness $\pm 7.5\%$ of the peak value in order to be in agreement with the original derivation of the analysis. In particular, three lamellar thicknesses were examined in detail, 185, 200, and 215 Å. The corresponding rates of unfolding, k_1 , for crystals of such dimensions are $1.9 \times 10^{-4} \text{ s}^{-1}$, $6.2 \times 10^{-6} \text{ s}^{-1}$, and $2.0 \times 10^{-7} \text{ s}^{-1}$, respectively. These varying rates of unfolding were used in the simulations to predict the effect of crystal size on the overall dissolution kinetics. The half thickness of the polymer slab was 0.35 mm, which was representative of the films prepared. In addition, the effect of the slab thickness on the overall dissolution kinetics was predicted by examining half thicknesses of 1 and 2 mm.

The crystal dissolution process was first examined in terms of changes in the crystalline structure over a period of 1 h of swelling for initial gels containing crystals of varying lamellar thickness. Fig. 7 shows the results obtained for the crystalline volume fraction as a function of time for samples of 185, 200, and 215 Å lamellar thickness. It is apparent from these results that the initial dimensions of the crystal significantly influenced the overall dissolution kinetics. Crystals of larger dimensions were much more stable as indicated by the nearly constant crystalline volume fraction for the 215 Å sample over 1 h of swelling. However, crystals of lower lamellar thickness of 185 Å demonstrated extremely rapid crystal unfolding and dissolution. Within 10 min, all of the crystals were predicted to melt out as shown by the crystalline volume fraction reaching zero. It is also interesting to note that a constant decrease

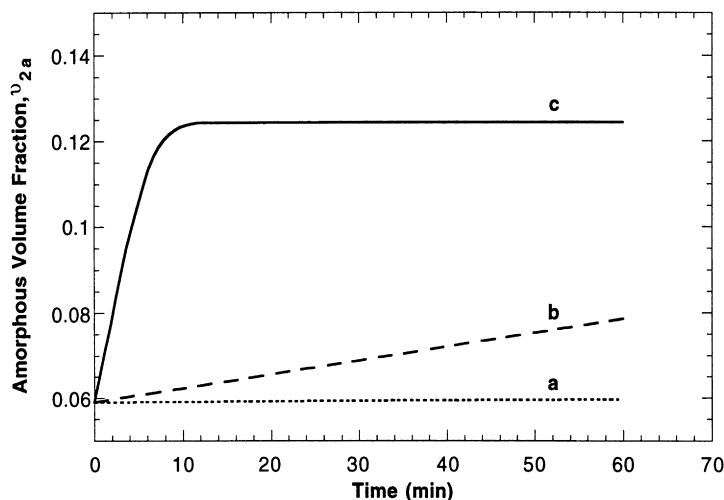


Fig. 8. Amorphous volume fraction as a function of time for samples containing crystals of lamellar thickness of (a) 215 Å; (b) 200 Å; and (c) 185 Å.

in the crystalline volume fraction over this period of 1 h was predicted for the peak lamellar thickness value. Essentially, if the PVA system were to be modeled as a polymer sample containing a uniform distribution of crystals of 200 Å, a constant decrease in the crystallinity would be expected until complete dissolution occurred. Obviously, these results show the significance of the distribution of crystal size in accurately modeling the overall behavior of freeze/thawed PVA gels.

Similarly, the changes in the amorphous volume fraction over this period of 1 h of swelling were predicted as shown in Fig. 8. The rapid unfolding of the 185 Å crystalline regions accounts for the drastic 6% increase in the amorphous fraction over a 10 min period of time. Again, we can see that the crystals of higher lamellar thickness showed little increase in amorphous PVA chains in the system. Such results emphasize the increased stability associated with crystalline regions of larger dimensions. In particular,

a relatively small change in the size of a crystal can significantly impact the overall dissolution kinetics.

This analysis demonstrated the influence of crystalline size on the rate of unfolding and subsequent dissolution behavior. In the previous results (Figs. 7 and 8) the kinetics were predicted in terms of three different systems with each containing a uniform distribution of crystals of 185, 200, or 215 Å. However, PVA gels prepared by freezing and thawing techniques contain a distribution of such crystals. Therefore, to predict the dissolution process of the system as a whole, an averaging technique was implemented. Essentially, the relative amounts of crystals at each lamellar thickness were determined using a representative distribution of crystals. The model system was determined to contain approximately 46% of crystals of 185 Å, 26 % of 200 Å, and 28% of 215 Å. Using such an analysis, the overall change in the crystalline volume fraction based on a distribution of crystals was determined as a function of time as

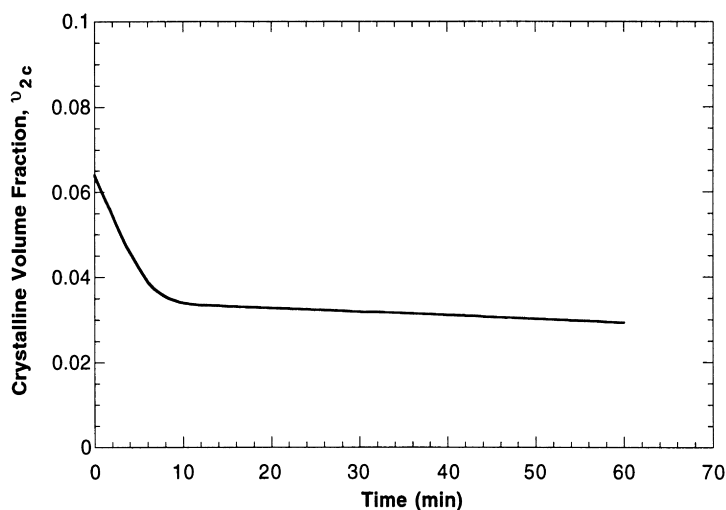


Fig. 9. Average crystalline volume fraction as a function of time for samples containing a distribution of crystals of varying lamellar thickness.

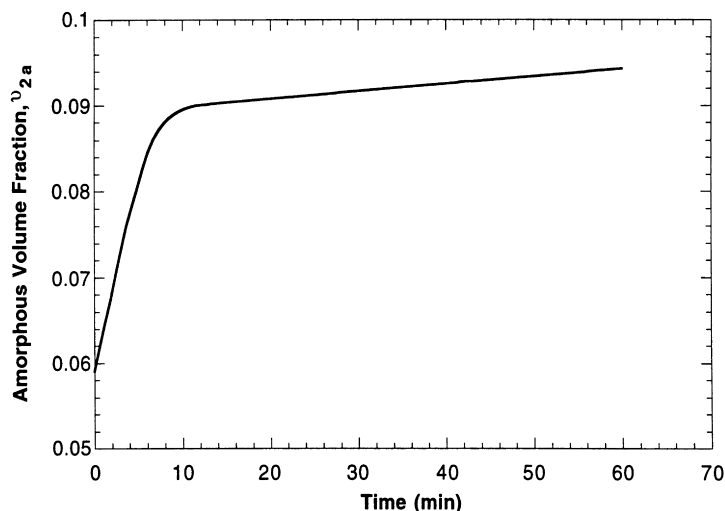


Fig. 10. Average amorphous volume fraction as a function of time for samples containing a distribution of crystals of varying lamellar thickness.

shown in Fig. 9. It is apparent that the model freeze/thawed PVA gel was predicted to show an initial rapid decrease in the crystalline volume fraction of approximately 3% in the first 10 min. However, the crystalline volume fraction did level off after this point with a continued relatively slow decrease. From these results it can be concluded that the presence of crystals of higher lamellar thickness serve to significantly stabilize the PVA system as a whole.

It is important to note that this model does not take into account the additional crystallization that may occur within the polymer system. This phenomenon can be demonstrated more closely by examining the change in the crystal size distribution during swelling as was shown in Fig. 4. Secondary crystallization was apparent as shown by a shift in the peak lamellar thickness and the introduction of crystals of higher lamellar thickness than were present in the original sample. Although a continued decrease in the crystalline

volume fraction over time was observed in Fig. 9, we would actually expect the system to better achieve a steady state due to the stabilizing effect of the crystals of larger dimensions that are introduced into the network during swelling. Overall, the model did predict a final crystalline volume fraction of approximately 0.03. This is in agreement with actual experimental results where the final crystalline volume fraction was determined to be approximately 0.04 upon swelling in water at 37°C. The discrepancies observed are likely due to the additional crystallization that occurs with freeze/thawed PVA gels during swelling.

The overall change in the amorphous volume fraction was also predicted by implementing the averaging technique with the estimated distribution of crystals. An overall increase in the amorphous volume fraction from 0.06 to 0.095 was predicted as shown in Fig. 10. The majority of the increase occurred during the first 10 min as the PVA

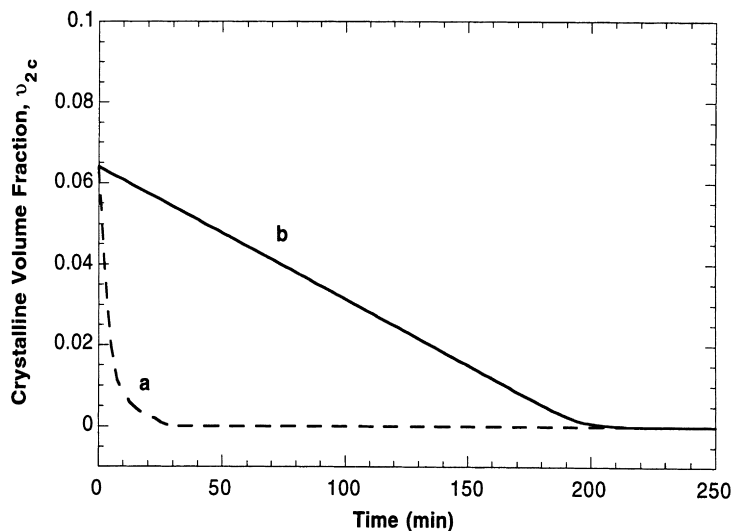


Fig. 11. Crystalline volume fraction over long times for samples containing crystals of lamellar thickness of (a) 185 Å and (b) 200 Å.

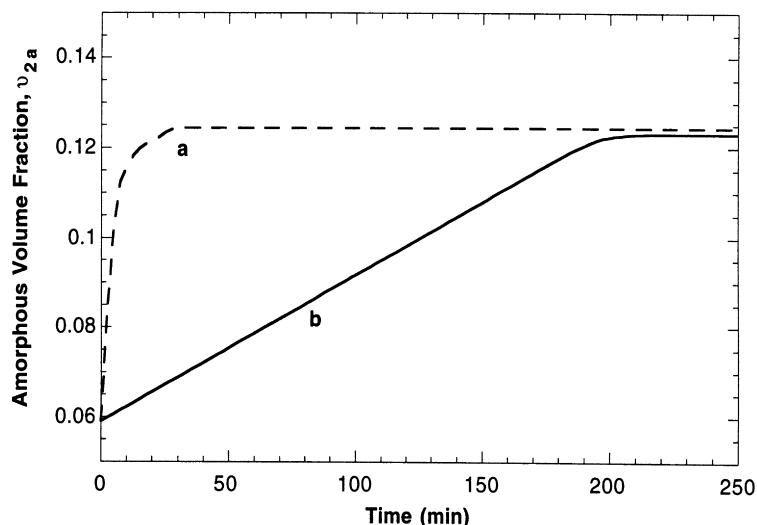


Fig. 12. Amorphous volume fraction over long times for samples containing crystals of lamellar thickness of (a) 185 Å and (b) 200 Å.

chains of the smaller crystalline regions unfolded at a rapid rate to join the amorphous portion. Again, there was a continued increase in the amorphous portion of the system that was more pronounced than what occurred in freeze/thawed PVA gels that actually exhibited some secondary crystallization that was not predicted by this model.

It was also of interest to examine the overall dissolution process over longer times of swelling. The behavior was examined over a period of 250 min for samples of 185 and 200 Å. The changes in the crystalline volume fraction are shown in Fig. 11. These results more closely show the drastic decrease of the crystalline volume fraction to zero in the first 10–20 min of swelling for crystalline regions of 185 Å. A more gradual melting out of crystalline regions of 200 Å thickness occurred over 200 min. In Fig. 12, the corresponding changes in the amorphous volume fraction

are shown. It is important to note here that a sample containing crystals of higher lamellar thickness not only demonstrated a more gradual increase in the amorphous volume fraction, but also achieved a final amorphous volume fraction that was slightly lower than that of the sample of 185 Å crystals. Although this difference is not very drastic, the implications should be considered particularly if the parameters were varied more significantly. Therefore, the lamellar thickness of the crystals not only affected the rate of dissolution, but also the final amorphous content within the structure.

The gradient of the amorphous fraction of the sample through the half slab was also examined (Fig. 13). It is apparent that with the lower lamellar thickness sample that there was a slight gradient of the amorphous volume fraction. In particular, a higher content of amorphous PVA

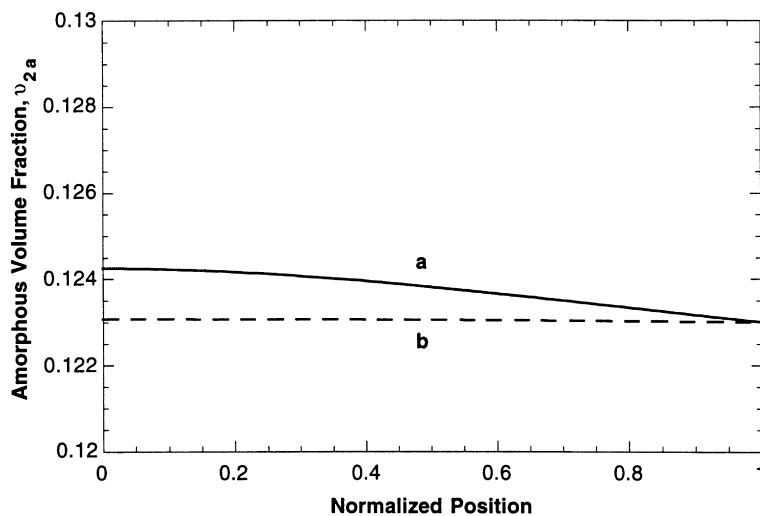


Fig. 13. Amorphous volume fraction as a function of position from the center of a slab for samples containing crystals of lamellar thickness of (a) 185 Å and (b) 200 Å.

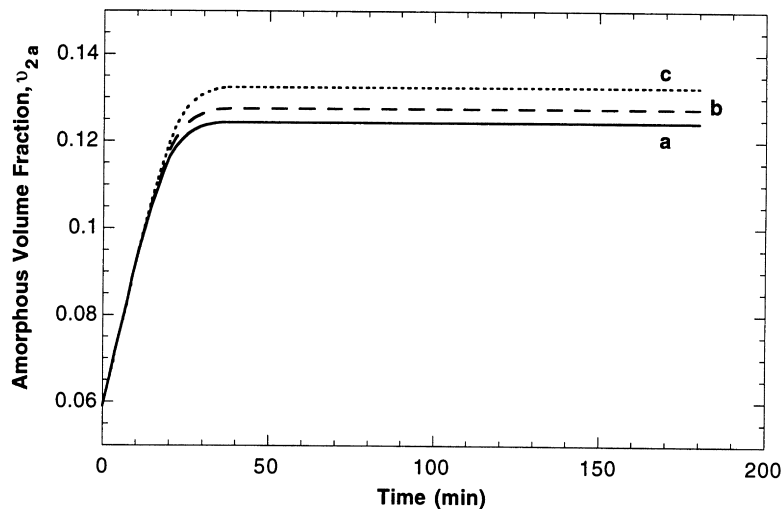


Fig. 14. Amorphous volume fraction as a function of time for varying slab thickness of (a) 0.35 mm; (b) 1.0 mm; and (c) 2.0 mm.

was predicted for the center of the slab than at the edge. Although this effect was quite small, it is expected to be more pronounced especially with lower crystal size and/or higher slab thickness.

To examine the effect of the slab thickness in more detail, simulations were performed for samples of crystal lamellar thickness of 185 Å with varying half slab thicknesses of 0.35, 1.0, and 2.0 mm. The amorphous volume fraction is shown as a function of time for these three samples in Fig. 14. It is apparent from these results that with a slab of increased thickness, there was an overall increase in the amount of amorphous PVA within the gel upon swelling. To further characterize the effect of the slab thickness, the amorphous volume fraction is shown as a function of the normalized position from the center of the slab (Fig. 15). Essentially, with increased slab thickness, a higher overall content of amorphous PVA in the center of the slab was predicted. These results demonstrate that a more uniform

structure in terms of amorphous and crystalline volume fractions are predicted for the swelling of thin slabs of freeze/thawed PVA.

5. Conclusions

The presence of crystals of higher lamellar thickness was predicted to be extremely important in the overall stability of PVA gels prepared by freezing and thawing techniques. This was observed through an averaging technique to represent an appropriate distribution of crystals. Final crystalline volume fractions correspond with the experimental results of such freeze/thawed gels. The model does have limitations in that the additional crystallization during swelling, or secondary crystallization, was not considered. This phenomenon, if incorporated into the model, would contribute to the stabilization of the system. However, the model

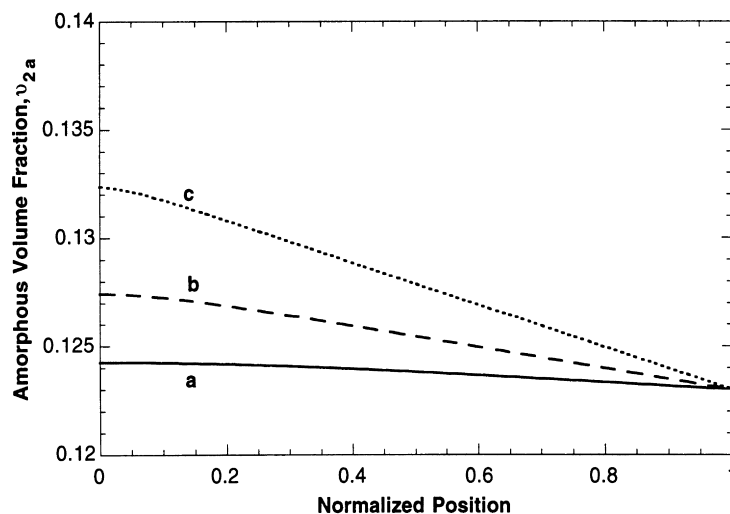


Fig. 15. Amorphous volume fraction as a function of position from the center of a slab for varying slab thickness of (a) 0.35 mm; (b) 1.0 mm; and (c) 2.0 mm.

implemented did provide good insight as to the effect of the lamellar thickness, the time of swelling, and the thickness of the sample on the crystal chain unfolding and potential dissolution of freeze/thawed PVA hydrogels.

Acknowledgements

This work was supported by grant GM-56231 from the National Institutes of Health and by a National Science Foundation Fellowship (to J.H.W.).

References

- [1] Peppas NA. In: Peppas NA, editor. *Hydrogels in medicine and pharmacy*, vol. 2. Boca Raton, FL: CRC Press, 1987. p. 1–48.
- [2] Tamura K, Ike O, Hitomi S, Isobe J, Shimizu Y, Nambu M. *Trans Am Soc Artif Organs* 1986;32:605–8.
- [3] Bao QB, Higham PA. US Patent 5,047,055, September 10, 1991.
- [4] Noguchi T, Yamamuro T, Oka M, Kumar P, Kotoura Y, Hyon SH, Ikada Y. *J Appl Biomater* 1991;2:101–7.
- [5] Cha WI, Hyon SH, Ikada Y. *Kobunshi Ronbunshu* 1991;48(7):425–30.
- [6] Hyon SH, Cha WI, Ikada Y, Kita M, Ogura Y, Honda Y. *J Biomater Sci Polym Ed* 1994;5:397–406.
- [7] Kuriaki M, Nakamura K, Mizutani J. *Kobunshi Ronbunshu* 1991;48(7):425–30.
- [8] Mallapragada SK, Peppas NA. *AIChE J* 1997;43:870–6.
- [9] Peppas NA, Merrill EW. *J Polym Sci: Polym Chem* 1976;14:459–64.
- [10] Glasstone S, Laidler KJ, Eyring H. *The theory of rate processes*. New York: McGraw-Hill, 1941.
- [11] Schultz JM. *Polymer materials science*. Englewood Cliffs, NJ: Prentice-Hall, 1974.
- [12] Kenney JF, Holland VF. *J Polym Sci: Part A-1* 1966;4:699–705.
- [13] Peppas NA, Hansen PJ. *J Appl Polym Sci* 1982;27:4787–97.
- [14] Fujita H. *Fortschr Hochpolym-Forsch* 1961;3:1–47.